Modeling of Micro Level Solar Radiation Using High Resolution Topographic Data through Remote Sensing and GIS

Samanta, S.,[1] Pal, D. K.[1] and Palsamanta, B.[2]
[1]Department of Survey and Land Studies, University of Technology, Papua New Guinea, LAE-411
E-mail:rsgis.sailesh@gmail.com, sailesh.samanta@pnguot.ac.pg , dkpal200090@gmail.com
[2]University of Technology Campus, Papua New Guinea, LAE-411, E-mail: mundey2@gmail.com

Abstract
In the current climate change scenario every nation is looking forward to taking control of their greenhouse emissions as a mitigation measure. Rapid exploitation of renewable energy and energy competence has culminated in significant energy safety and self-reliance for the fossil fuel importing countries, apart from climate change mitigation and economic benefits. Availability of solar radiation data is essential in order to evaluate the potential of renewable energy options such as photovoltaic power generation capability in a developing economy like Papua New Guinea. Installation of roof top solar panels can easily generate electricity without affecting the environment. So this research is an initiation to identify potential roof-tops for installation of solar panel. Therefore a micro level solar radiation modeling is attempted using high resolution topographic database for four spatial days and four different months, like March, June, September and December. ArcGIS spatial analyst, model builder and raster calculator tools are used to prepare solar radiation database through a GIS-based solar radiation model. Different essential parameters like latitude, elevation, slope and aspect, viewshed, sky map, sun map and atmospheric condition in terms of aerosol content induced transmitivity are taken into account for micro level solar radiation modeling. The modeled output data set represents global radiation or total amount of incoming solar insolation in kilo watts per square meter (Kw/m^2/day) calculated for pixel-by-pixel of the input surface. The resulted output database highlights average monthly global radiation of 5.34 KW/m^2/day in the month of March, 4.00 KW/m^2/day in June, 5.25 KW/m^2/day in September and 5.15 KW/m^2/day in December. As expected in a country of southern hemisphere, the output map indicates higher solar radiation in the north facing roof of buildings than other parts of the roof as well as the road and open area. Shaded zones can be easily identified as no direct solar radiation is available over those places. With the help of the expected energy output computed rationally, such type of study can be useful for identifying optimal sites for roof-mounted solar panels for captive electricity generation.

1. Introduction

Incoming solar radiation (insolation) remains the driver of most fundamental patterns of weather and climate (Fu and Rich, 2002). Insolation reaching earth surface depends on a number of factors e.g. atmospheric chemistry, latitude, altitude, slope, aspect, duration or day-length, seasonal distribution, landscape pattern (Cristobal et al., 2005). Differential thermal inertia of objects on the earth surface also causes uneven heating responsible for the vertical as well as horizontal motion of the wind. Formation of cloud is the result of such wind carrying sufficient moisture from surface waters; former causing profound variation of insolation reaching earth surface, the former also being aggravated by the country's sustained proximity to Inter-tropical convergence zone (ITCZ). Thus the differential insolation over space and time should be taken cognizance of toward estimation of plausible power output using photovoltaic panels at a particular geographic location. In Papua New Guinea CO_2 emissions from the combustion of fuels are projected to reach 15.2 million tonnes by 2030, which is a massive 337% increase from the 1990 level of 4.5 million tonnes (APERC, 2009). Rapid exploitation of renewable energy and energy competence result in significant energy safety, climate change mitigation, and economic benefits (IEA, 2012).

At present the most of the rural communities within Papua New Guinea (PNG) do not enjoy electricity (Samanta and Aiau, 2015). Although a far cry, Government of Papua New Guinea (GoPNG) is looking into green avenues of increasing the power capacity across the country to meet 2050

ISSN 1686-6576 / © Geoinformatics International

millennium set goals (PNG Vision 2050) of zero net emission. Pyranometer data provide ground-based Global Horizontal Irradiance (GHI) values for solar potential assessment (Martínez et al., 2009 and PV-Tech, 2015).Researchers have found 10-15 uncertainty in the satellite-based GHI estimation (PV-Tech Power, 2015 and Peruchena and Amores, 2017). Many models such as Heliosat-4 (Qu et al., 2017), REST2 (Gueymard, 2008) have been developed by researchers to assess the solar potential. Apart from these models many researchers adopted different methodology for modeling of solar radiation, where they mentioned that relief is the major parameter in a particular geographical location (Samanta et al., 2016, Turton, 1987 and Ododo et al., 1996). Use of empirical correlation functions to translate sunshine duration into global radiation values is the possible solution in the modeling of solar radiation (Ododo et al., 1996, Fan et al., 2019, Jin et al, 2005 and Ampratwum and Dorvlo, 1999). Fuzzy logic can be used to compute global radiation from sunshine duration (Sen, 1998). It is also possible to compute radiation from cloud cover and sunshine duration (Supit and Van Kappel, 1998).

Lae city is currently experiencing frequent load shadings (a term used to describe zone-wise power black-outs in rotation to match the shortfall in generation) and will be continuing throughout the year which was mentioned in a press release by PNG Power Limited (PPL). Electricity supply to Lae city from Ramu hydro power station was disconnected due to high demand and low generation capacity. Currently Daewoo's diesel power station at Munum just outside of Lae is supplying the power and is not enough as per demand of the city and uptown settlements. In the recent past solar lights were installed in the side of many streets (about 16 streets) of the Lae city that nicely light up the streets and minimized the heap of power bills of Lae city council (The National, 2013). So the renewable energy like solar energy is the alternative source for electricity supply to the city with zero emission.

Installation of roof top solar panel can easily generate electricity without affecting the environment. In this scenario, the GIS-based micro level solar radiation modeling is attempted using very high resolution topographic information generated from remote sensing data. The beauty of remote sensing lies in its ability to generate primary data in user required scale, which is easily accessible and is very handy. Airborne Light Detection and Ranging (LiDAR) is an optical remote sensing technology that provides extremely accurate, high-resolution elevation data.

This study aims to GIS-based solar radiation modeling based on high resolution topographic data. The main objective of this research is to model topographic solar radiation values at a micro level scale. This research was conducted in the Lae city which is the capital city of Morobe province. The main advantages of this research is to model solar radiation at the micro-scale using high resolution topographic data from which ideal sites for solar panel placement on building rooftops can be determined, while such goal is impossible to achieve using low resolution gridded data.

2. Study Location

Even with the help of a very efficient machine, insolation calculations for a high resolution digital elevation model (DEM) can take hours, and very high resolution topography data could take days. As it is very much time consuming, two small sites within Lae city under Morobe province of Papua New Guinea are selected for this experimental research work. Lae city, known as the industrial city of the country, is the second largest city of Papua New Guinea and is the capital city of Morobe province situated near to the mouth of Markham River (Figure 1). Circle shaped study site-1 is about 4.67 hectares of land with a center coordinate of 146° 59′ 06.66″ E and 6° 44′ 03.16″ S and is located in between Montoro street and Erica street. The study site-2 is located between Mash street and Marsina street and it covers an area of 6.67 hectares with the center coordinates of 146° 59′ 22.42″ E and 6° 44′ 21.79″ S.

3. Data Sets Used for the Study

Different types of datasets are used for calculation of solar radiation, output verification, authentication and distribution map preparation of solar variables within the study area. National Aeronautic and Space Agency (NASA) does release Surface meteorology and Solar Energy (SSE) database (v. 6.0) through its' Earth science research program (Stackhouse and Whitlock, 2008). This data base (SSE 6.0) contains more than 200 primary and derived solar, meteorology and cloud related parameters from data across the 22 year period (1983 - 2005). SSE parameters are downloaded from its user-friendly web-based portal in gridded format. This data is available on a 1° by 1° equal-angle grid covering the entire globe (Stackhouse and Whitlock, 2009). Clear sky insolation, clear sky insolation clearness index, transmittivity factor and diffuse proportion have been considered for modeling of solar radiation (Samanta et al., 2016).

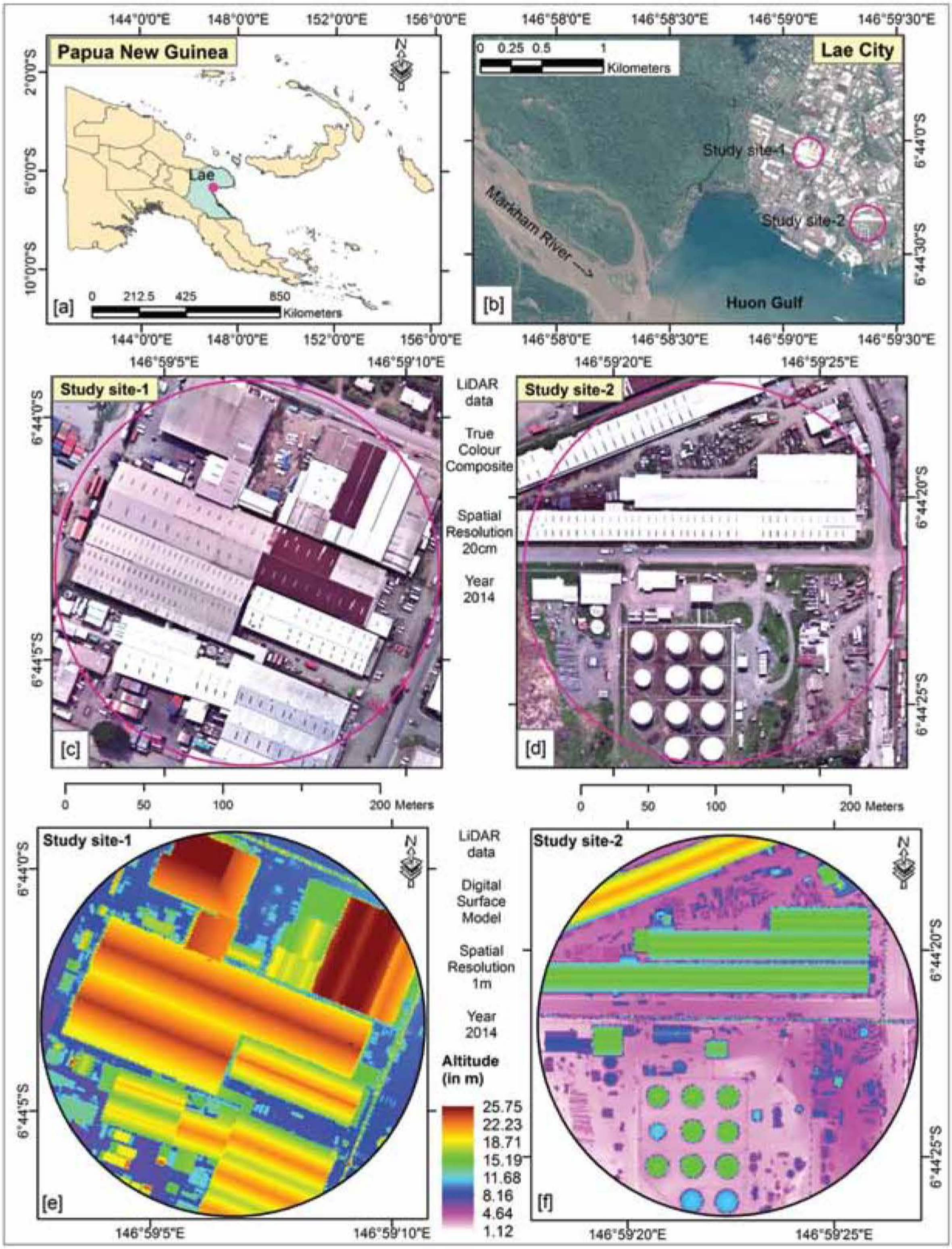

Figure 1: Location map of the study area; Papua New Guinea [a], Lae city in the mouth of Markham with study sites [b], satellite view of study site 1 [c] and study site 2 [d], and surface elevation of study site 1 [e] and study site 2 [f]

Table 1: Data sets used for solar radiation calculation model

Sl. No.	Data Description	Data type/ Resolution	Year	Source
1	Clear sky insolation, Clear sky insolation clearness index,	1° grid	1983- 2005	Surface meteorology and Solar Energy (SSE, v. 6.0) https://eosweb.larc.nasa.gov/sse
2	Average global solar radiations, diffuse and direct radiation			
3	Aerial Imagery	20 cm	2012	Department of Surveying and Land Studies, Papua New Guinea University of Technology
4	Digital elevation model (DEM)	1 m		
7	Digital surface model (DSM)	1 m		

Other important variable of SSE database depicting global averaged solar radiations which contain both diffuse and direct radiation have been considered to validate model output of this research and to find the error of estimation that cropped out through this GIS based solar radiation estimation model.

High resolution topographic data and aerial imagery was captured via airborne LiDAR surveys during May-July 2012. Four towns, namely Vanimo, Wewak, Madang and Lae, as well as the connecting coastal strips were surveyed to underpin future coastal planning and management activities (PACCSAP, 2012). Airborne LiDAR measures distances by sending a pulse of light from a laser towards the area being surveyed. The laser and sensor are mounted on a specialist aircraft in which a GPS system is used for positioning (PACCSAP, 2012). Aerial imagery of 20 cm spatial resolution, digital elevation model (DEM) in 100 cm (1 m) spatial resolution and digital surface model (DSM) of surface features such as tops of buildings, trees and bare ground are used into the GIS based solar radiation calculation model as important input parameters. Both DEM and aerial imagery for site-1 and site-2 are cropped from original processed data sets using ArcGIS spatial analyst tools. The study details of the data sets used in this research are given in Table 1.

4. Methodology

DSM data set with the spatial resolution of 100 cm (1 m) for the selected study sites was used as an essential input into the GIS based solar radiation model (Fu and Rich, 2000, 2002 and Samanta et al., 2016). The model used other relevant parameters to calculate the variation of micro level solar radiation, namely solar constant, solar elevation, solar azimuth angle, the distance between Earth-Sun, sun incident angle to each raster cell, slope and aspect, viewshed, zenith division, azimuth divisions, sky map sector, sun map sector, diffuse proportion and finally transmitivity of the atmosphere. ArcGIS spatial analyst, model builder and raster calculator tools were used to solve solar radiation equations (equation 1 to equation 3) (Fu and Rich, 2000, 2002 and Samanta et al., 2016). Global solar radiation ($Global_{tot}$) is the sum of direct radiation (Dir_{tot}) and diffuse radiation (Dif_{tot}) as in equation 1.

$$\mathrm{Global_{tot}} = \mathrm{Dir_{tot}} + \mathrm{Dif_{tot}}$$

Equation 1

Direct radiation ($Dir_{\theta,\alpha}$) was calculated based of solar constant, atmospheric transmitivity, Sun duration, Sun gap fraction and angle of incidence between the sky sector and the surface based on equation 2.

$$\mathrm{Dir}_{\theta,\alpha} = S_{\mathrm{const}} \quad \beta^{m(\theta)} \quad \mathrm{SunDur}_{\theta,\alpha} \quad \mathrm{SunGap}_{\theta,\alpha} \quad \mathrm{Cos}(\mathrm{AngIn}_{\theta,\alpha})$$

Equation 2

Where, S_{Const} stands for Solar flux; β is atmospheric transmitivity; $^{m(\theta)}$ is the relative optical path length; $SunDur_{\theta,\alpha}$ is the time duration represented by the sky sector; $SunGap_{\theta,\alpha}$ is the gap fraction for the sun map sector; and $AngIn_{\theta,\alpha}$ is the angle of incidence between the sky sector and the intercepting surface.

Finally diffuse radiation can be reached to the surface after redirecting radiation from all visible parts of the sky. Diffuse radiation ($Dif_{\theta,\alpha}$) was calculated based *diffused normal radiation flux*, the time interval, proportion of visible sky and angle of incidence using Equation 3.

$$\mathrm{Dif}_{\theta,\alpha} = P_{\mathrm{dif}} \quad \mathrm{Dur} \quad \mathrm{SkyGap}_{\theta,\alpha} \quad \mathrm{Cos}(\mathrm{AngIn}_{\theta,\alpha}) \quad \mathrm{Weight}_{\theta,\alpha} \quad R_{\mathrm{glb}}$$

Equation 3

Where: P_{dif} is the proportion of global normal radiation flux that is diffused; Dur is the time interval for analysis, $SkyGap_{\theta,\alpha}$ is the gap fraction for the sky sector, $AngIn_{\theta,\alpha}$ is the angle of incidence between the sky sector and the intercepting surface; R_{glb} is the global normal radiation; $Weight_{\theta,\alpha}$ is the *proportion of diffuse radiation originating in a given sky sector relative to all sectors.*

The solar constant used in the analysis is 1367 W/m^2 based on world radiation center (WRC) solar constant (Samanta et al., 2016). The ratio between global solar radiation at ground level and extra-terrestrial solar radiation is called as atmospheric transmitivity or clearness index or atmospheric transmission coefficient. The transmitivity of the atmosphere depends on density of air mass, the amount of water vapour as the most variant principal greenhouse gas, aerosol present and the relative optical path length (Fu and Rich, 2000). The average distance between Earth and Sun is about 149.6 million km with a closest distance of 147.3 million km on 3rd January (perihelion) and longest distance to 152 million km on 4th July (aphelion) (Yang and Vidal, 1990).

The angle between the earth-sun line and the earth's equatorial plane is called angle of declination which differs from day to day. Two angles that describe the alignment of Sun to Earth locations are the solar altitude and the solar azimuth (Fu and Rich, 2000). Solar altitude is normally measured from either the southern or northern point along the horizon and begins at zero degrees (Pidwirny, 2006). Maximum solar altitude occurs when the Sun is directly overhead and has a value of 90°. The differential altitude at solar noon (north or south leaning) in different latitudes is owing to the two solstices and equinoxes (Table 2). Viewshed analysis is essential to calculate the direct, diffuse and total radiation to each cell. The viewshed refers to the portion of sky which is viewed from a particular location. A sunmap displays the sun track, or apparent position of the sun with respect to a given geographical location. It varies from time to time, like different hours of a day and different days of the year. Diffuse radiations received at a particular location are attributed to scattering of solar radiation by atmospheric components of the hemispherical sky, depending on path length and chemistry of the atmosphere. For modeling of diffuse radiation for a location, skymap is required which represents a hemispherical view of the entire sky (Fu and Rich, 2000). It can be divided into a numbers of sky sectors based on zenith and azimuth angles.

The mean latitude of - 6.7365° south based on the input surface rasters of the study area is considered for the modeling purpose. Slope and aspect of the study area are calculated from high resolution DSM and were used as inputs in this model. Another optional parameter is sky size or resolution, which is considered as 500 cells per side for the viewshed, skymap, and sunmap rasters in the solar radiation calculations. One hour time interval through the day-length was used for calculation of sky sectors for sun maps. The modeling was initiated to estimate monthly average solar radiation for special days (June Solstice, 2 Equinoxes: vernal and autumnal, and December Solstice) and months (March, June, September and December) for the year 2018. Finally zenith division, azimuth divisions, diffuse model type, transmitivity and diffuse proportion parameters were used as radiation input parameters into the model.

The number of zenith and azimuth directions was allied to the spatial resolution of DSM. 16 azimuth and 16 zenith directions were applied for the model. One of the previous researches (Butt et al., 2014) provided a proper explanation how satellite cloud data can be used as inputs to the diffuse radiation model to provide estimates of annual and monthly diffuse radiation proportion. Fraction of insolation at the top of the atmosphere which reaches the surface of the earth is clear sky insolation clearness index. Based on NASA-SSE data set monthly average (23 years: 1983 to 2006) clear sky insolation clearness index for the study area is 0.715.

Table 2: Maximum Sun altitudes (in degrees) for selected latitudes

Latitude (in degrees)	March 21 (Vernal Equinox)	June 21 (Summer Solstice of North hemisphere)	September 23 (Autumnal Equinox)	December 21 (Summer Solstice of South hemisphere)
0 °	90 °	66.5 °	90 °	66.5 °
23.5 S	66.5 °	43 °	66.5 °	90 °
50 S	40 °	16.5 °	40 °	63.5 °
60 S	30 °	6.5 °	30 °	53.5 °
66.5 S	23.5 °	0 °	23.5 °	47 °
70 S	20 °	-3.5 °	20 °	43.5 °
90 S	0 °	- 23.5 °	0 °	23.5 °

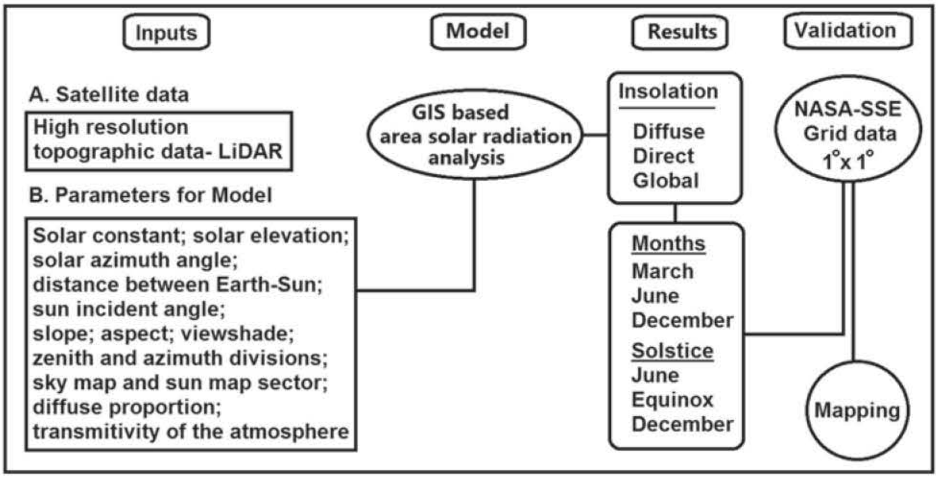

Figure 2: Workflow of the micro level solar radiation modeling

Table 3: Average direct, diffuse and global insolation in special days and months

Radiation Type and Duration	Mar	Jun	Sep	Dec	June Solstice	Equinox	Dec Solstice
Diffuse ($KW/m^2/day$)	1.35	1.16	1.34	1.33	1.14	1.33	1.33
Direct ($KW/m^2/day$)	3.98	2.85	3.91	3.82	3.00	4.05	3.91
Global ($KW/m^2/day$)	5.34	4.00	5.25	5.15	4.14	5.38	5.24
Duration (Hrs)	9.75	8.69	9.58	9.90	9.18	10.06	10.19

The clear-sky transmitivity of most tropical regions in general seems to lie between 0.68 and 0.75 (Louis and Sunday, 2003 and Godfrey and Anthony, 2014). For Papua New Guinea value of 0.35 is used in this study as diffuse proportion and 0.55 as transmitivity are considered because of preponderance of cloudiness and overcast sky typical of tropical rainforest regions. The overview of the workflow is shown in Figure 2.

5. Result and Discussion

Viewshed database was developed from high resolution DSM data using 3D analyst tool of ArcGIS. All pixels of the resulting viewshed were assigned a value that represents to whether the sky direction is visible or obstructed (Rich et al., 1994). The viewshed (hemispheric) was generated in 16 azimuth direction for the solar radiation calculation because of sudden variation of surface due to use of high resolution DSM (Figure 3). The sun track was calculated based on the latitudinal positions and the time configuration that defines sunmap sectors. Gap fraction, the proportion of unobstructed sky area in each skymap or sunmap sector, is calculated by dividing the number of unobstructed cells by the total number of cells in that sector (Figure 3a). Figure 3b represents approximate position of the Sun for each one hour period of the day ranged from June 21 to December 21, 2018. The skymap of half-hour period of the day in specific months and year and sunmap with 16 zenith and 16 azimuth divisions was generated through spatial analyst tools of ArcGIS with the help of high resolution DSM data and overlaid with the viewshed layer (Figure 3c, 3d) to calculate direct radiation(Samanta et al., 2016). The modeled output data set represents incoming solar insolation in kilowatt hours per square meter per day ($KW/m^2/day$) calculated for pixel-by-pixel of the input surface. Basic three (3) types of solar insolation were mapped, namely (i) diffuse insolation, (ii) direct insolation and (iii) global insolation.

Average monthly diffuse radiation was recorded highest at 1.35 $KW/m^2/day$ in the month of March compared to other months (Table 3). Similarly average monthly direct radiation was also higher during month of March, about 3.98 $KW/m^2/day$. Month of June experienced lowest average monthly diffuse radiation and direct radiation at 1.16 $KW/m^2/day$ and 2.85 $KW/m^2/day$ respectively. The study area received highest average monthly global radiation at almost 5.34 $KW/m^2/day$ in the month of March compared to 4.00 $KW/m^2/day$ in June, 5.25 $KW/m^2/day$ in September and 5.15 $KW/m^2/day$ in December (Table 3). While comparing among special days, diffuse, direct and global radiation are much more during Equinoxes (21st March and 23rd September) than that during Solstices, because Sun come overhead during these special days and also because of the study area's proximity to the

Equatorial lows or the Inter-Tropical Convergence Zone (ITCZ). This is substantiated by the fact that the global radiation was calculated at 5.38 $KW/m^2/day$ during both Equinoxes. As expected, the output maps (Figure 4) indicate higher solar radiation in the north facing roof of the buildings than other parts of the roof as well as the road and open area during Equinoxes and the June solstice, whereas higher solar radiation was calculated in the south facing roof of buildings.

The study indicates that the overall average solar radiation is higher on the roofs with northerly aspects.

Figure 5 represents monthly global solar radiation for three months, December, March and June at site-1 and site-2. Maximum global solar radiation was calculated as 6.33 $KW/m^2/day$ on December solstice and average maximum global solar radiation during month of December in the south facing roof tops.

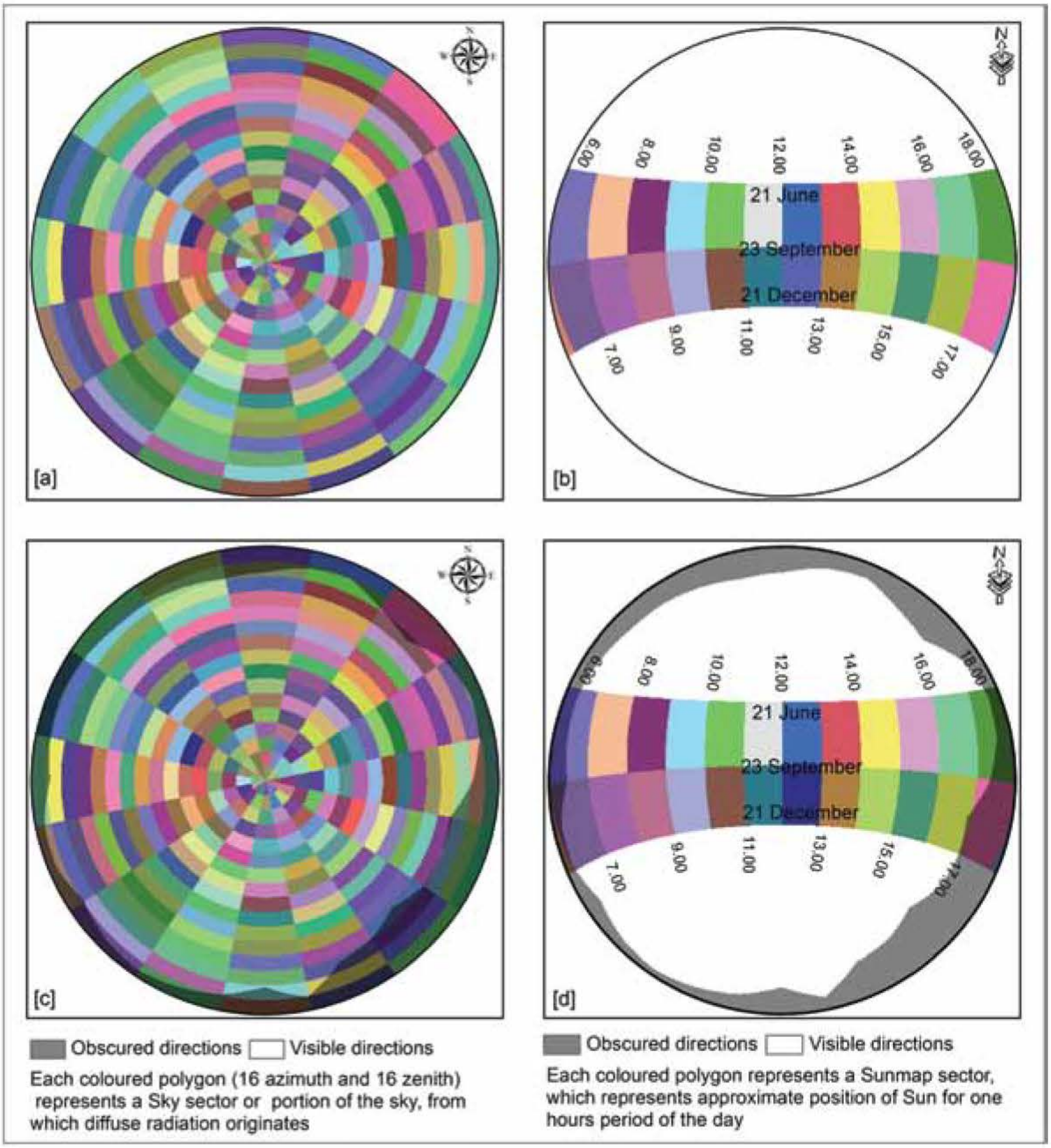

Figure 3: Hemispherical skymap [a], sunmap [b] and schematic overlay of skymap on viewshed [c] and skymap on viewshed [d]

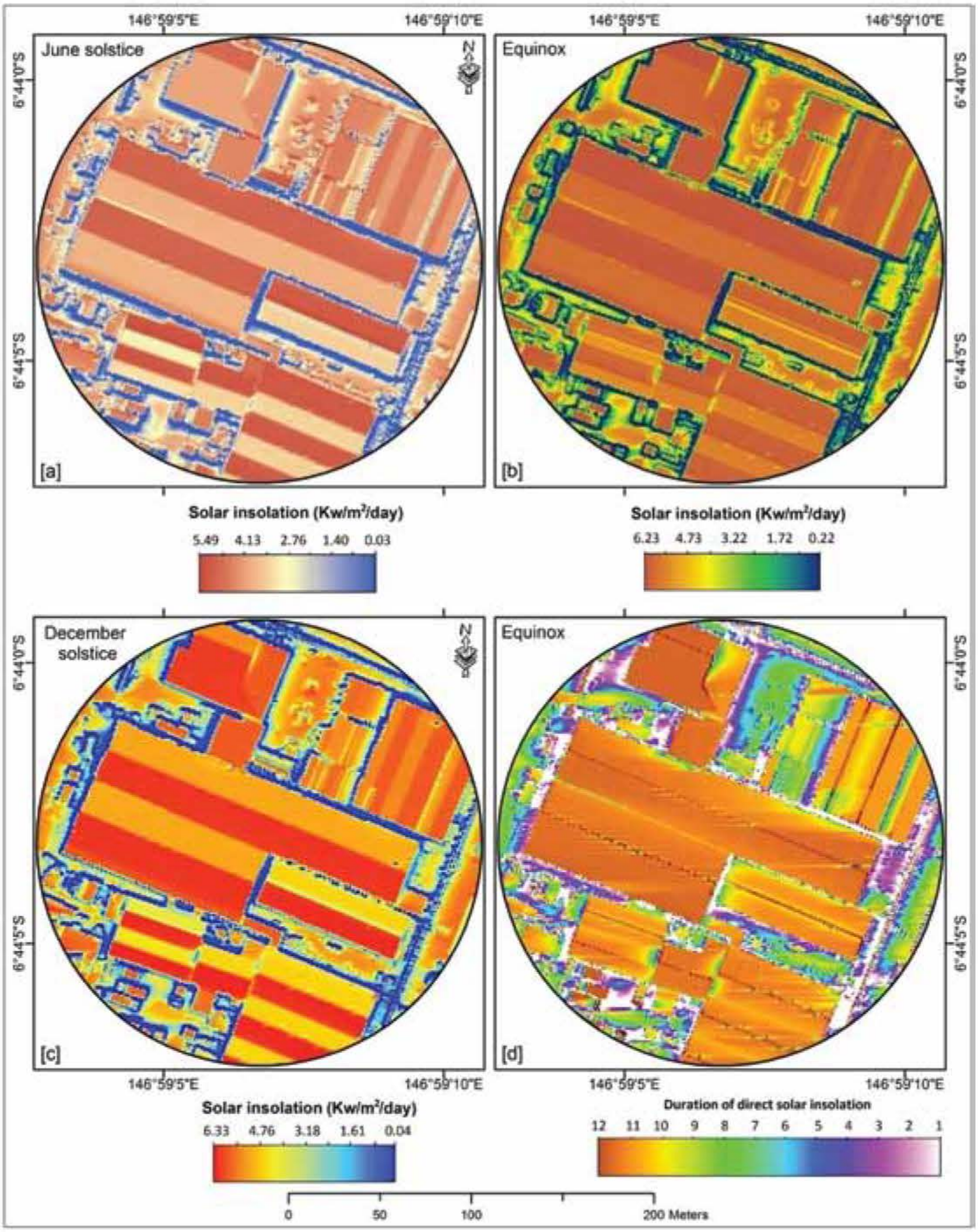

Figure 4: Global solar radiation during special days: June solstice [a], Equinox [b] December solstice [c] and duration of direct radiation during Equinox [d]

Table 4: Comparison of solar radiation between NASA-SSE and GIS based solar model output

Insolation unit: KW/m²/day					
Measurement type	**March**	**June**	**September**	**December**	**Average**
NASA-SSE @ 146°30' E; 6°30' S	5.03	4.46	5.02	5.22	4.93
RS & GIS based @ Lae	5.34	4.00	5.25	5.15	4.94
Correlation coefficient (r)	0.923				
Regression coefficient (R^2)	0.851				

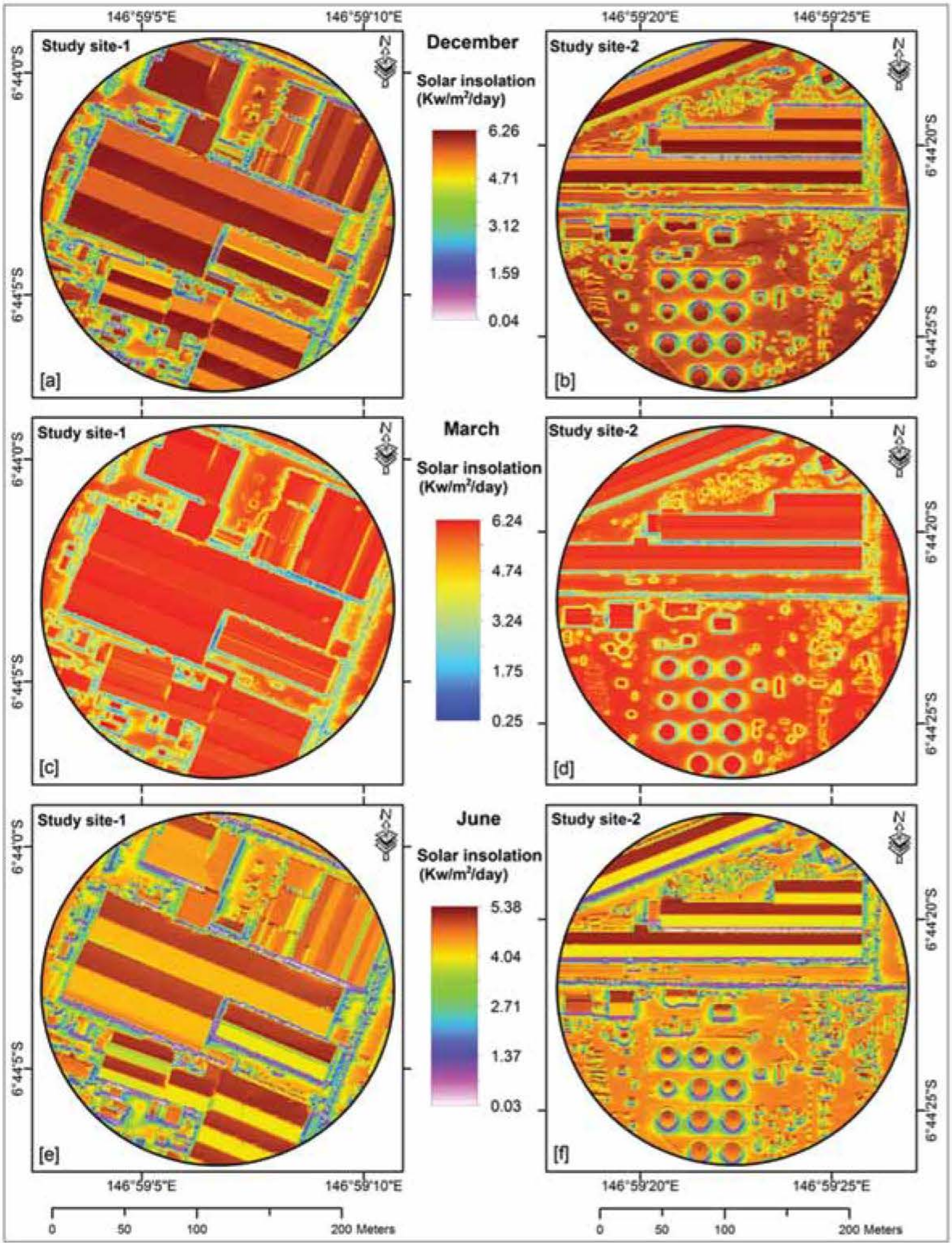

Figure 5: Global solar radiation during months of December [a], [b]; March [c], [d]; and June [e], [f] for study site 1 and 2

This is the time when distance between Sun-Earth is much closer than other special dates and months when the sun shines in the southern hemisphere creating a favorable situation for the south facing and roofs of tall buildings to receive more radiations instantly. While considering average monthly global radiation both Equinoxes and month of March receive higher radiation than other solstices and months (Table 3). Duration of direct incoming solar radiation was calculated at 9.90 hours during the month of December which is higher than other months and 10.19 hours during December Solstice that happens to be much higher than June Solstice (Table 3). Shaded zones can be easily identified as very little direct solar radiation zones available over those places. The areas between two buildings are indicated as low duration direct insolation zones than the top roof of a building or elevated places in the study sites (Figures 4 and 5).

Result of this GIS based solar model was compared with NASA-SSE gridded data (1° x 1°) to validate modelled output. While comparing with NASA Surface meteorology and Solar Energy (SSE) data sets, we received good prediction with correlation coefficient value of 0.923 and a Regression coefficient of 0.851 (Table 4). As there are no ground based station available in this region, we used NASA-SSE gridded data as an alternative option. Advantage of this research is the use of high resolution topographic data (1m x 1m) into the GIS based solar model. Mapping of potential solar irradiance is required to map more realistically, especially at the micro-scale level, since rooftop structure may impact PV system performance and power generation capacity. In this scenario NASA-SSE gridded data (1° x 1°) is very coarse database in comparison to our micro level modelling using high resolution topographic data.

6. Conclusion

The Govt. of PNG is committed to achieving electrification of houses of its 70% population by 2030 from the current dismal figure of only 13%. It is an expectation of very tall order, as such its realisation is extremely challenging. When the population density of the country is very low and also is highly scattered through rugged terrains, the installation of national-wide grid and connecting every houses will be an extremely difficult and prohibitively expensive task. Thus the only alternative is to create isolated, captive power generation units. Given this background, the generation of micro-level solar installations could be of paramount significance. The proposed methodology allows computing solar radiation values on the Earth surface on a monthly and daily basis giving valuable results using a very high-resolution digital Surface model. The result of the study will be a boon in fostering the cost-benefit analysis of such installations. This type of research on solar insolation modelling might enthuse researchers towards a better understanding of climate change scenarios, which keeps affecting the most for the fragile economies of small island countries like PNG. This study is expected to come handy for planners to install solar panels in the roof of buildings for captive electricity generation.The major limitation of this research is to handle high volume of high resolution topographic data into the system, which takes a day or two to execute the model equation. Secondly there were no ground based stations that can generate datasets for verification of this GIS-based solar model output. Recently the department Electrical Engineering of Papua New Guinea University of technology has constructed a ground based station at Umi Township, Markham valley in Morobe province and data are likely to be collected and stored for research purpose. These ground based measurement data can be used to validate the RS/GIS model output. In extension of this current case study our recommendation is to continue further research on void-free high resolution topographic data complimented with station data from larger geographical area.

References

Ampratwum, D. B. and Dorvlo, A. S., 1999, Estimation of Solar Radiation from the Number of Sunshine Hours. *Applied Energy*, Vol. 63, 161-167.

APERC, 2009, *Asia Pacific Energy Research Centre, APEC Energy Demand and Supply Outlook*, 4th Edition, Papua New Guinea, Economic Review, 76-80.

Butt, N., New, M., Malhi, Y., Costa, A.C.L., Oliveira, P. and Silva-Espejo, J. E., 2010, Diffuse Radiation and Cloud Fraction Relationships in Two Contrasting Amazonian Rainforest Sites. *Agricultural and Forest Meteorology*, Vol. 150, 361-368.

Cristobal, J., Pons, X. and Ninyerola, M., 2005, Modelling Actual Evapotranspiration in Catalonia (Spain) by Means of Remote Sensing and Geographical Information Systems. *Gottinger Geographische Abhandlungen*, Vol.113, 144-150.

Fan, J., Wu, L., Zhang, F., Cai, H., Zeng, W., Wang, X. and Zou, H., 2019, Empirical and Machine Learning Models for Predicting Daily Global Solar Radiation from Sunshine Duration: A Review and Case Study in China. *Renewable and Sustainable Energy Reviews,* Vol. 100, 186-212.

Fu, P. and Rich, P. M., 2000, The Solar Analyst 1.0 Manual, *Helios Environmental Modeling Institute (HEMI)*. USA.

Fu, P. and Rich, P. M., 2002, A Geometric Solar Radiation Model with Applications in Agriculture and Forestry. *Computers and Electronics in Agriculture,* Vol. 37, 25-35.

Godfrey, N. O. and Anthony, O. C. N., 2014, Relationship between Global Solar Radiation and Sunshine, Hour Duration for Bida in Nigeria. *International Journal of Renewable and Sustainable Energy,* Vol. 3 (2), 43-46. doi: 10.11648/j.ijrse.20140302.12.

Gueymard, C.A., 2008, REST2: High-Performance Solar Radiation Model for Cloudless-Sky Irradiance, Illuminance and Photosynthetically Active Radiation - Validation with a Benchmark Dataset. *Sol Energy*, Vol. 82, 272-285.

IEA, 2012, International Energy Agency. Energy Technology Perspectives, 2012. Archived from the Original on 6 July 2015, https://www.iea.org/publications/freepublications/publication/ETP2012_free.pdf

Jin, Z., Yezheng, W. and Gang, Y., 2005, General Formula for Estimation of Monthly Average Daily Global Solar Radiation in China. *Energy Conversion and Management*, Vol. 46(2), 257-268.

Louis, E. A. and Sunday, E. E., 2003, Relationship between Global Solar Radiation and Sunshine Duration for Onne, Nigeria. *Turk J Phys,* Vol. 27, 161-167.

Martínez, M, A., Andújar, J. M. and Enrique, J.M., 2009, A New and Inexpensive Pyranometerfor the Visible Spectral Range. *Sensors (Switzerland),* Vol. 9, 4615-4634.

Ododo, J. C., Agbakwuru, J.A. and Ogbu, F. A., 1996, Correlation of Solar Radiation with Cloud Cover and Relative Sunshine Duration. *Energy and Conversion Management*, Vol. 7(10), 1555-1559.

PACCSAP, 2012, Pacific-Australia Climate Change Science and Adaptation Planning (PACCSAP) program, International Climate Change Adaptation, PNG LiDAR Factsheet, https://www.pacificclimatechange.net/sites/default/files/documents/LiDAR-PNG.pdf

Peruchena, C. F. and Amores, A.F., 2017, Uncertainty in Monthly GHI Due to Daily Data Gaps.*Sol Energy*, Vol. 157, 827-829.

Pidwirny, M., 2006, Earth-Sun Geometry. *Fundamentals of Physical Geography. 2nd Edition*, UBC Okanagan, online at: http://www.physicalgeography.net.

PNG Vision-2050, 2009, Papua New Guinea Vision-2050, National Strategic Plan Taskforce, Government of Papua New Guinea, http://actnowpng.org/sites/default/files/png%20version%202050.pdf

PV-Tech Power, 2015, The art and Science of Pyranometers. PV-Tech Power, Vol. 3, 48-51, https://www.pv-tech.org/pv-tech-power/pv-tech-power-volume-3

Qu, Z., Oumbe, A., Blanc, P., Espinar, B., Gesell, G., Gschwind, B., Klüser, L., Lefèvre, M., Saboret, L., Schroedter-Homscheidt, M. and Wald, L., 2017, Fast Radiative Transfer Parameterisation for Assessing the Surface Solar Irradiance: The Heliosat-4 Method. *Meteorol Zeitschrift*, Vol. 26, 33-57.

Rich, P. M., Ralph, D., William, A. H. and Shawn, C. S., 1994, Using Viewshed Models to Calculate Intercepted Solar Radiation: Applications in Ecology. *American Society for Photogrammetry and Remote Sensing Technical Papers*, 524-529.

Samanta, S. and Aiau, S.S., 2015, Spatial Analysis of Renewable Energy in Papua New Guinea through Remote Sensing and GIS, *International Journal of Geosciences*, Vol. 6, 853-862. doi. 10.4236/ijg.2015.68069

Samanta, S., Pal, D. K., Aiau, S. S. and Palsamanta, B., 2016, Geospatial Modeling of Solar Radiation to Explore Solar Energy Potential in Papua New Guinea. *Spatial Information Research*, Vol. 24(5), 531-544. 10.1007/s41324-016-0050-x.

Sen, Z., 1998, Fuzzy Algorithm for Estimation of Solar Irradiation from Sunshine Duration. *Solar Energy*, Vol. 63, 39-49.

Stackhouse, P. W. and Whitlock, C. H.,(eds) 2009, Surface meteorology and Solar Energy (SSE), Release 6.0 Methodology, NASA SSE 6.0, Earth Science Enterprise Program, NASA, Langley, https://eosweb.larc.nasa.gov/sse/documents/SSE6Methology.pdf

Supit, I. and Van Kappel, R.R., 1998, A Simple Method To Estimate Global Radiation. *Solar Energy*, Vol. 63, 147-160.

The National, 2013, https://www.thenational.com.-pg/solar-to-light-up-lae-streets/

Turton, S.M., 1987, The Relationship between Total Irradiation and Sunshine Duration in the Humid Tropics. *Solar Energy*, Vol. 38, 353-354.

Yang, C. and Vidal, A., 1990, Combination of Digital Elevation Models with SPOT-1 HRV MultispectralImagery for Reflectance Factor Mapping. *Remote Sensing of Environment*, Vol. 32, 35-45.